Available online at www.sciencedirect.com
ScienceDirect
Geochimica et Cosmochimica Acta 72 (2008) 3170–3183
Geochimica et Cosmochimica Acta
www.elsevier.com/locate/gca

Heating experiments on glass inclusions in Allende (CV3) olivines: Clues to the formation conditions of chondrules?

Maria Eugenia Varela *

Complejo Astronómico El Leoncito (CASLEO), Av. España 1512 sur, J5402DSP San Juan, Argentina

Received 10 October 2007; accepted in revised form 21 April 2008; available online 1 May 2008

Abstract

Several pieces of the Allende CV3 chondrite were heated up to different final temperatures (1100, 1250, 1450 °C) with the aim to study glassy and glass-bearing inclusions in olivines as well as the glass mesostasis of chondrules and aggregates. The experiments were performed in a Pt-Pt90Rh10 heating stage at 1 bar pressure. The oxygen fugacity is estimated to have been between 10^{-9} and 10^{-10} atm at 1200 °C. The variation of the chemical composition of the heated glasses gives information concerning the behavior of the incompatible elements (with respect to the host) Al, Ca and Na. The chemical variation in the heated mesostasis glass shows that Ca exchange between the gas and condensed phases at sub-solidus temperatures can occur in a short time. Laboratory heating experiments show that glass inclusions will behave as closed systems and therefore preserved the alkalis they acquired. On the other hand, the mesostasis glass can loose them when heated to temperatures higher than 1100 °C. Evidently, the presence of Na-rich glasses, in chondrules and aggregates available to us, indicate that if there was a thermal process that did affect them, it must have been a low temperature one.

1. INTRODUCTION

Glass inclusions represent small volumes of liquids enclosed by a host mineral during its growth. Heating experiments on glass inclusions allow reversing the post-entrapment processes that occurred inside the inclusions during cooling. These experiments—performed on glassy and glass-bearing inclusions—make possible to obtain information regarding the conditions prevailing during host formation, either in terrestrial or extra-terrestrial rocks (e.g., Fuchs et al., 1973; Sobolev et al., 1976; Clocchiatti and Massare, 1985; Varela et al., 2000; Schiano, 2003). Here I report on the heating experiments performed on glass inclusions in olivines and mesostasis glass from the Allende CV3 chondrite. The accent of these experiments is placed in the behavior of the incompatible elements (e.g., for the host olivine) like Ca and Na. Both elements can reach high concentrations in glasses of glass inclusions and mesostasis in the olivine-rich objects of chondritic meteorites (Varela et al., 2002a, 2005, 2006), but are particularly interesting in the Allende chondrules. This interest is due to the fact that our previous studies show that, although scarce, some glasses in Allende Dark Inclusions (DI) and Allende host—that are not only rich in Al but also in Na—qualify as possibly being primitive glasses (Varela et al., 2002b).

Consequently, some glass compositions of inclusions in Allende olivine seem to be primitive, suggesting that Na was available at the moment of formation of the inclusions. As has been suggested (Varela et al., 2002b) during formation of these glasses temperatures must have been low enough (950 K) to allow condensation of small amounts of Na_2O into the glasses without altering their Ca/Al chondritic ratio.

Because heating experiments were performed on natural objects up to different final temperatures (1100, 1250, 1450 °C), the variation in the chemical composition of glasses of open (e.g., mesostasis) and closed (e.g., glass inclusions) systems can serve to better constrain the processes taking place during and after chondrule and/or aggregate formation.

* Fax: +54 264 4213693.
E-mail address: evarela@casleo.gov.ar

0016-7037/$ - see front matter © 2008 Elsevier Ltd. All rights reserved.
doi:10.1016/j.gca.2008.04.018

2. SAMPLES AND ANALYTICAL TECHNIQUES

Heating experiments were performed with a double-polished section of the Allende meteorite (PTS, Naturhistorisches Museum, Vienna) at the Laboratoire Pierre Süe, CEA, Saclay, France. The thickness of the section—of around 100–200 μm—allows the selection of olivine-rich objects with glass inclusions by with an optical microscope. From the selected chondrules (round, droplet-shaped objects) and/or aggregates (irregularly shaped angular to rounded object) a small piece (less than 1 mm in size) was extracted for the heating experiments.

Major element compositions of glasses were measured with a Camebax CAMECA and a SX100 Cameca electron microprobe (Centre d'analyses Camparis, Université de Paris VI and University of Vienna, respectively) using an accelerating voltage of 15 kV and a sample current of 10 nA. A defocused beam (5–7 μm) or scanning areas of 10 × 10μm where applied for glass inclusions and mesostasis glasses, respectively, while a focused beam was used for minerals. In order to reduce loss of Na during analysis this element was analyzed first with a counting time of 5 s. The detection limit for minor elements is as follow: Na_2O: 0.05, K_2O: 0.03, P_2O_5: 0.04, MnO: 0.02. Analytical scanning electron microscopy was performed with a JEOL-6400 instrument (NHM, Vienna), with a sample current of 1 nA and an acceleration voltage of 15 kV.

The precision for the elements was established by replicate analyses of basaltic and rhyolitic standard glasses (ALV 981 R24 and CFA 47; Métrich and Clocchiatti, 1989).

Heating experiments were performed in a Pt-Pt90Rh10 heating stage at 1 bar pressure in a hot He atmosphere as oxygen getter (Zapunnyy et al., 1989). The sample is placed in a heating stage attached to a petrographic microscope, which allows direct observation during a single heating run. The heater consists of a 6 mm long vertical tube within which the sample is placed for observation with transmitted light. The doubly polished surface permits a more defined transmitted light optical observation even for sample 4 to 5 orders of magnitude thicker than the usual petrographic thin section. The sample holder is of 1 mm diameter on which is placed a thick plate (100–300 μm) of a mineral used as sample carrier, over which is placed the polished piece of the sample (<1 mm in size) to be investigated. The sample carrier used in all runs was a doubly polished round plate of San Carlos olivine (Fig. 1). The gas mixture Ar–H_2 (1% H_2) fluxing imposed an oxygen fugacity of 10^{-9} and 10^{-10} atm at 1200 °C that is directly measured using a zirconia probe.

Quenching times were less than 1 s. The system was calibrated at the melting point of Au (1064.43 °C). Runs were of 8 h each with increasing heating rates as follow: 5 °C/min up to 300 °C, 2–3 up to 700 °C and 1–2 °C/min from this temperature to the final temperature of 1100, 1250 and 1450 °C, respectively. The final temperatures were held during 2 h (with exception of a second run at 1250 °C which was held during 24 h) after which a rapid quench (less than 1 s to about 500 °C) preserved the final conditions (Table 1). After these experiments the polished section is mounted in resin and polished until the glass inclusions and mesostasis glasses under investigation are exposed to the surface (Fig. 3).

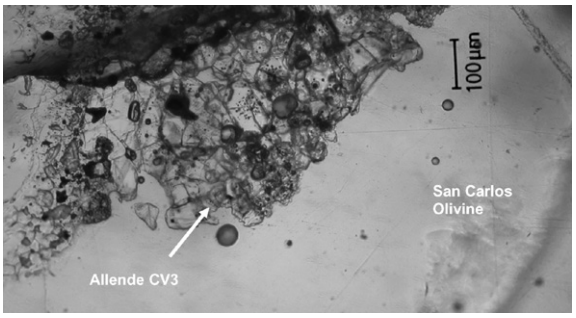

Fig. 1. Optical image of the double-polished thin piece of an aggregate from the Allende CV3 chondrite on a round plate (100–300 μm) of San Carlos olivine used as sample carrier.

Table 1
Experimental conditions

Heating runs	Room temp. to 300 °C	300–700 °C	700 °C to FT
Increasing heating rates (°C/min)	5	2–3	1–2
Final temperature (FT) (°C)	1100	1250	1450
Duration of each run (h)	8	8	8
Time keeping the FT (h)	2	2 and 24	2
Quenching (s)	<1	<1	<1

3. RESULTS

3.1. Petrography and chemical composition of glasses

Inspection of the section before heating experiments under the optical microscope allowed selection of chondrules and/or aggregates with a PO texture, as both types of olivine-rich objects show a high abundance of primary glass inclusions. Once the objects were isolated from the section, a small part of them (<1 mm) was selected from the center of the object. In both types of selected objects glasses occur as: (a) primary glass inclusions or glass-bearing multiphase inclusions in olivines and, (b) as mesostasis glasses (Fig. 2). The sizes of the primary glass inclusions selected for electron microprobe (EMP) analyses were around 10 μm or bigger, to avoid host contamination. EMP analyses of olivines that host glass inclusions, were done close to the location of the glass inclusions.

In CV chondrites, chondrules and aggregates commonly do not contain glassy mesostasis, but consist of holocrystalline assemblages, that are usually altered (e.g., Ikeda and Kimura, 1995). Thus, the heating experiments will try to reverse the post-entrapment reactions that effectively occur in natural objects during cooling giving rise, for example, to a re-crystallized mesostasis. Re-melting experiments will preserved an approximate view of how the coexisting assem-

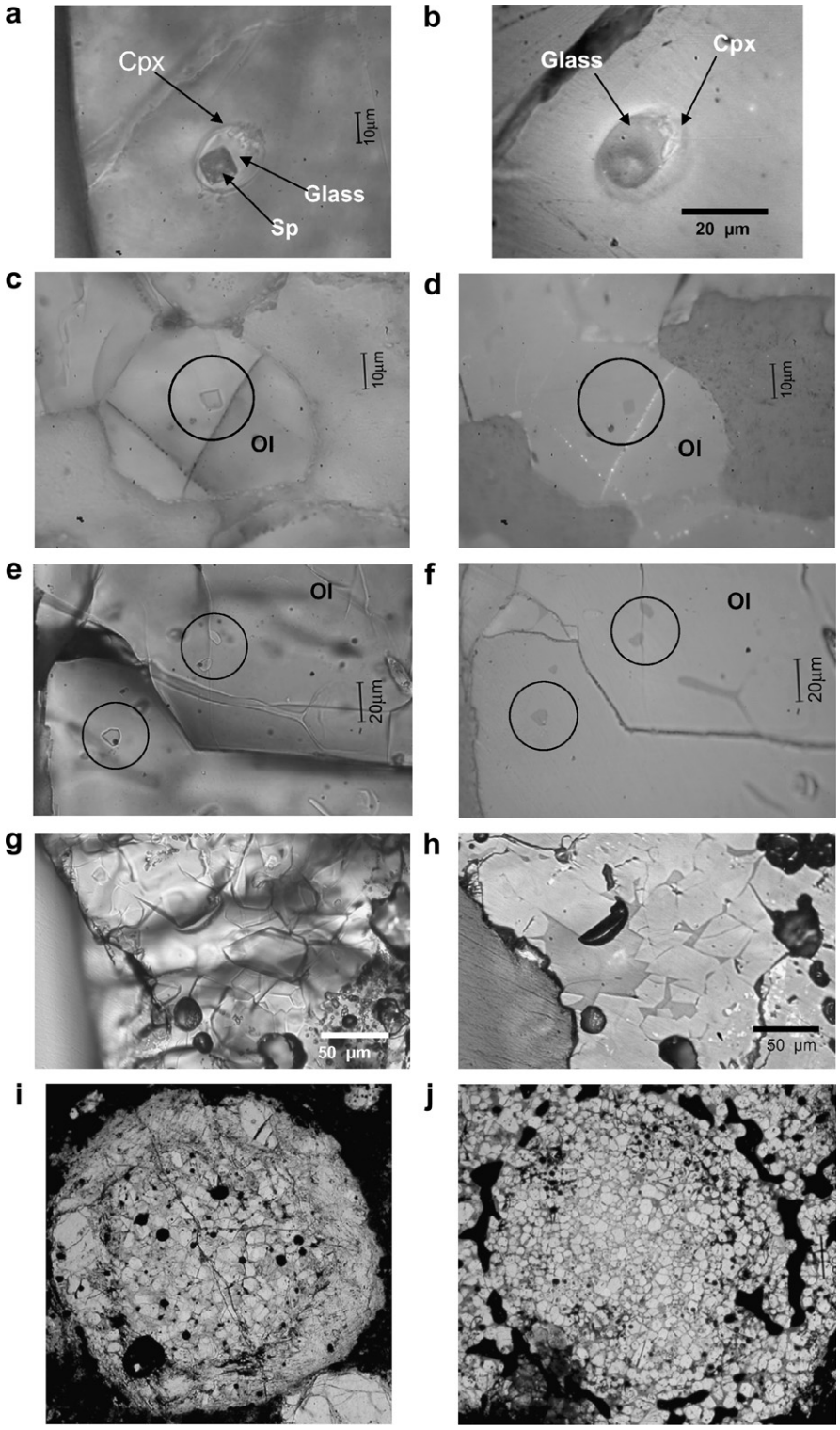

Fig. 2. (a) Transmitted and (b) reflected light optical image showing the multiphase inclusion with the euhedral spinel crystal, the coexisting glass and the clinopyroxene. (b) Note that the spinel crystal remains below the sample surface. Sample heated to a final temperature of 1100 °C. (c) Transmitted and (d) reflected light optical image of an isolated euhedral glass inclusion in olivine. Sample heated to a final temperature of 1200 °C. (e) Transmitted and (f) reflected light optical image of three glass in olivine. Sample heated to 1250 °C and held during 24 h. (g) Transmitted and (h) reflected light optical image of mesostasis glass in olivine aggregate from the Allende chondrite. Sample heated to a final temperature of 1250 °C and held during 24 h. Transmitted light optical image of PO chondrules with (i) clear (diameter of the object 750 μm) and (j) re-crystallized mesostasis.

blage of phases looked at the imposed final temperature of each run. A quenching time of less than 1 s will preserved these conditions and allows the study of glassy mesostasis, which are rare in the Allende chondrules available to us.

The petrographic inspection of the sample was performed on the heated samples, once the olivine-rich objects were re-polished and all phases (e.g., glass inclusions, host olivines and mesostasis) were exposed to the surface.

All studied glasses (e.g., glass inclusions and mesostasis) looked clean without signs of devitrification.

The chemical composition of unheated glasses of glass inclusions in olivines of the Allende meteorite varies as follow: SiO_2: 42.9–55.9 wt%; TiO_2: 0.00–1.64 wt%; Al_2O_3: 19.3–30.8 wt%; FeO: 0.00–4.15 wt%; MgO: 0.31–3.45 wt%; CaO: 1.5–24 wt%; Na_2O: 0.55–14.8 wt%; K_2O: 0.00–0.96 wt%.

The CIPW norm (as wt% norm) for the mean value of 82 unheated glass inclusions (Table 2) is: plagioclase: 68.13; orthoclase: 0.83; nepheline: 10.82; diopside: 10.81; wollastonite: 9.19; ilmenite: 1.77; apatite: 0.35.

The glasses of the mesostasis were analyzed in two different PO chondrules. In one of them (Fig. 2i) the mesostasis is a clear glass without signs of devitrification (labeled as: c, Table 2). In the second object (Fig. 2j) the mesostasis is completely re-crystallized (labeled as: ∗, Table 2). The chemical composition of the clear mesostasis varies as follow: SiO_2: 44–44.6 wt%; TiO_2: 0.01–0.09 wt%; Al_2O_3: 33.2–33.8 wt%; FeO: 0.68–0.92 wt%; MgO: 0.49–2.65 wt%; CaO: 17.7–18.5 wt%; Na_2O: 0.79–1.14 wt%. The major elemental composition of five olivines in contact with the clear mesostasis varies as follow: SiO_2: 41.7–43.8 wt%; FeO: 3.55–4.1 wt%; MgO: 51.1–54.2 wt%; CaO: 0.26–0.52 wt%.

Table 2
Representative major element composition of glasses of unheated glass inclusions in olivines (EMPA in wt%)

SiO_2	42.9	48.6	47.2	45.2	43.9	54.7	48.2	48.5	52.5	54.2	45.2	52.1	51.2
TiO_2	1.20	0.98	1.64	1.32	0.04	0.84	1.46	0.00	0.75	0.61	1.32	0.94	0.92
Al_2O_3	26.1	25.4	26.9	23.4	30.1	20.4	23.8	30.8	23.1	20.5	23.4	22.7	21.4
Cr_2O_3	0.05	0.16	0.91	0.11	0.27	0.57	0.57	0.01	1.09	0.11	0.11	0.59	0.82
FeO	0.28	1.25	0.76	0.23	4.15	0.08	0.59	1.33	0.34	0.40	0.23	0.49	0.10
MnO	<dl	<dl	<dl	0.02	0.02	0.02	0.07	<dl	<dl	0.08	0.02	0.02	0.04
MgO	0.57	3.82	0.40	3.31	3.04	0.31	1.79	1.23	0.40	0.91	3.31	0.30	1.85
CaO	23.4	17.1	15.4	24.0	1.5	13.2	13.7	15.9	15.5	11.8	24.0	16.7	14.7
Na_2O	4.31	2.86	6.6	0.55	14.8	7.8	8.6	2.38	6.6	10.1	0.55	6.6	8.7
K_2O	0.03	0.06	0.18	0.04	0.96	0.07	0.08	<dl	0.26	0.51	0.04	<dl	0.25
P_2O_5	0.22	0.15	0.08	0.26	<dl	0.14	0.17	0.18	0.17	<dl	0.26	0.19	<dl
Total	99.1	100.4	99.9	98.4	98.8	98.1	99.0	100.4	100.8	99.2	98.4	100.7	100.0
													M(82)
SiO_2	54.7	52.7	58.2	53.7	55.4	48.7	49.0	57.1	47.4	49.6	52.7	55.9	**52.0**
TiO_2	0.84	0.94	0.64	0.86	0.44	0.93	1.22	1.51	1.16	1.02	0.94	0.86	**0.92**
Al_2O_3	20.4	23.4	19.3	25.5	20.7	25.5	23.9	19.8	24.4	23.5	23.4	19.4	**22.99**
Cr_2O_3	0.57	0.71	0.56	0.99	0.41	0.50	0.51	0.62	0.74	0.31	0.71	0.49	**0.52**
FeO	0.08	0.28	0.92	0.55	0.70	0.18	0.63	0.61	0.09	0.00	0.28	1.05	**0.86**
MnO	0.02	0.09	0.03	0.05	0.02	0.03	<dl	<dl	0.07	0.14	0.09	<dl	**0.04**
MgO	0.31	0.31	1.02	1.70	1.13	1.80	1.40	1.67	0.53	3.45	0.31	1.89	**1.59**
CaO	13.2	13.0	10.6	7.2	10.2	12.2	10.7	13.9	18.0	11.6	13.0	11.1	**13.8**
Na_2O	7.8	7.5	8.6	9.0	10.2	9.7	10.4	3.7	6.7	9.6	7.5	9.3	**6.2**
K_2O	0.07	0.03	<dl	0.39	0.33	0.27	0.33	0.02	0.14	0.25	0.03	0.07	**0.14**
P_2O_5	0.14	0.16	0.12	<dl	<dl	0.13	0.13	0.22	0.25	0.09	0.16	0.08	**0.15**
Total	98.1	99.1	99.9	99.9	99.6	99.9	98.3	99.1	99.4	99.5	99.1	100.1	**99.2**

Mesostasis	C	C	C	C	C	∗	∗	∗	∗	∗	∗	∗	∗	∗	∗
SiO_2	44.3	44.3	44.5	44.0	44.6	43.4	45.1	50.2	53.4	53.8	53.2	50.2	53.1	53.9	55.3
TiO_2	0.02	0.02	0.09	0.01	0.06	0.90	1.01	0.91	0.98	1.05	1.06	0.91	0.97	1.04	1.05
Al_2O_3	33.8	33.7	32.1	33.7	33.3	20.0	21.3	21.0	23.9	23.9	23.8	21.0	22.9	23.9	24.8
Cr_2O_3	0.03	<dl	0.11	0.03	<dl	0.44	0.55	0.46	0.53	0.48	0.38	0.46	0.44	0.42	0.55
FeO	0.74	0.89	0.71	0.68	0.92	3.96	2.62	3.02	2.26	1.65	1.55	3.02	2.77	2.12	2.44
MnO	<dl	<dl	0.04	<dl	<dl	0.06	<dl	0.02	0.03	<dl	0.03	0.02	<dl	0.02	0.05
MgO	0.49	0.50	2.65	0.62	1.13	4.32	4.46	5.0	2.04	1.86	2.08	5.0	2.58	1.66	2.12
CaO	18.3	18.1	17.7	18.5	17.7	11.1	9.7	7.8	2.1	1.6	2.1	7.8	3.3	2.0	2.3
Na_2O	0.93	0.90	0.79	0.79	1.14	9.0	9.8	11.1	14.8	15.0	15.1	11.1	13.6	14.6	9.8
K_2O	<dl	<dl	<dl	<dl	<dl	0.41	0.47	0.11	0.04	0.07	0.09	0.11	0.03	0.08	0.06
Total	98.6	98.3	98.7	98.3	99.0	93.6	95.0	99.6	100.1	99.4	99.2	99.6	99.6	99.8	98.5

M (82), mean of 82 analyses; <dl, below detection limit.
Samples: Polish thin sections Allende A, Allende B, Allende Q and Allende M5618 from NHM (Vienna).
References: C, clear mesostasis; ∗, re-crystallized mesostasis.

The chemical composition of the re-crystallized mesostasis varies between: SiO_2: 43.4–55.3 wt%; TiO_2: 0.68–1.06 wt%; Al_2O_3: 21–24.8 wt%; FeO: 1.55–3.96 wt%; MgO: 1.66–5 wt%; CaO: 1.98–11.1 wt%; Na_2O: 9–15.1 wt%; K_2O: 0.03–0.47 wt%. That of the 12 olivines in contact with the re-crystallized mesostasis varies between: SiO_2: 40.2–42.3 wt%; FeO: 1.9–7.3 wt%; MgO: 51.1–56.1 wt%; CaO: 0.18–0.29 wt%.

The chemical composition of the glasses of 26 heated glass inclusions in olivines of the Allende meteorite, for a final temperature of 1100–1450 °C varies as follow: SiO_2: 46.2–69.6 wt%; TiO_2: 0.24–2.84 wt%; Al_2O_3: 8.3–22.1 wt%; FeO: 2.00–12.2 wt%; MgO: 5.8–19.4 wt%; CaO: 5.4–17.1 wt%; Na_2O: 0.00–7.8 wt% (Table 3). That of the mesostasis heated up to final temperatures of 1100–1450 °C, varies between: SiO_2: 46.2–54.4 wt%; TiO_2: 0.06–0.88 wt%; Al_2O_3: 11.5–33.6 wt%; FeO: 0.62–13.1 wt%; MgO: 0.4–15.1 wt%; CaO: 6.9–18.1 wt%; Na_2O: 0.00–1.43 wt% (Table 4).

One multiphase glass inclusion (composed of glass plus a euhedral spinel crystal) did develop some fibrous crystals (clinopyroxene) during heating that grew big enough to become visible at the final temperature of 1100 °C (Fig. 2a and b). The chemical composition of the clinopyroxene is as follow: SiO_2: 47.8 wt%; TiO_2: 1.87 wt%; Al_2O_3: 12.9 wt%; FeO: 1.16 wt%; MgO: 13.6 wt%; CaO: 22.6 wt%; Na_2O: 1.07 wt%. That of the glass—coexisting with the newly grown clinopyroxene and the pre-existing spinel—is: SiO_2: 49.5 wt%; TiO_2: 1.33 wt%; Al_2O_3: 17.1 wt%; FeO: 2.0 wt%; MgO: 9.9 wt%; CaO: 15.1 wt%; Na_2O: 4.96 wt% (Table 3).

In samples heated to a final temperature of 1100 °C the major elemental composition of eight olivines (three crystals host of glass inclusions and five in contact with a clear mesostasis) varies as follow: SiO_2: 40.7–41.8 wt%; TiO_2: 0.00–0.1 wt%; Al_2O_3: 0.01–0.2 wt%; FeO: 4.83–8.7 wt%; MgO: 50.6–54.2 wt%; CaO: 0.21–0.28 wt%. For those heated till final temperatures of 1250 °C, the major elemental composition of eight olivines (three crystals host of glass inclusions and five in contact with a clear mesostasis) varies between: SiO_2: 41.5–42.9 wt%; TiO_2: 0.00–0.05 wt%; Al_2O_3: 0.04–0.15 wt%; FeO: 3.13–8.7 wt%; MgO: 51.6–56.6 wt%; CaO: 0.13–0.33 wt%. In samples heated to a final temperature 1250 °C, which was held during 24 h, the major elemental composition of six olivines (three crystals host of glass inclusions and three in contact with a clear mesostasis) varies between: SiO_2: 39.5–41.6 wt%; TiO_2: 0.00–0.04 wt%; Al_2O_3: 0.00–0.1 wt%; FeO: 5.8–16.4 wt%; MgO: 44.8–53.4 wt%; CaO: 0.12–0.28 wt%. In samples heated to a final temperature of 1450 °C, the major elemental composition of seven olivines (two hosts of glass inclusions and five in contact with a clear mesostasis) varies between: SiO_2: 40.6–41.2 wt%; TiO_2: 0.00–0.05 wt%; Al_2O_3: 0.00–0.16 wt%; FeO: 9.2–13.1 wt%; MgO: 43.2–50.3 wt%; CaO: 0.22–0.33 wt%.

4. DISCUSSION

4.1. Heating experiments: a comparison

The very first heating experiments performed on glass inclusions in olivines from carbonaceous chondrites are those undertaken by Fuchs et al. (1973). The few preliminary experiments were done "at 100 °C intervals from 1200 to 1400 °C for periods of several hours followed by air-quenching to room temperature".

In the following paragraphs a comparison between the heating experiments performed on glass inclusions of the Murchison chondrite (Fuchs et al., 1973) and those from the Allende chondrite (this study) can help to better understand the conditions prevailing during formation of the glass inclusions and their hosts in these two types of chondrites.

Glasses of the glass inclusions in Allende olivine show no optical changes during heating. There was no sign of devitrification in the clear glass inclusions, as well as no change in those glasses that were already devitrified before the heating. In all glass inclusions but one, there were no detectable growing phases during heating. The exception is one glass inclusion that showed a reduction of the bubble size around 950 °C. After continued heating of the same inclusions to a final temperature of 1100 °C some clinopyroxene did develop (Fig. 2a and b). Previous heating experiments (Fuchs et al., 1973) also report, in few cases, the appearance of crystals during heating of the glass inclusions, which composition could not be established because they disappeared after heating to higher temperatures.

In the same inclusion where clinopyroxene did form (Fig. 2a and b), the euhedral spinel crystal, that was already present before the heating experiments, did not suffer any visible alteration. The chemical composition of the coexisting heated glass (label # in Table 3), has a CaO/Al_2O_3 ratio of 0.88 close to the chondritic ratio (CI: $CaO/Al_2O_3 = 0.8$). The fact that glasses of unheated multiphase (glass + spinel crystal + bubble) and spinel-free glass inclusions show also a CaO/Al_2O_3 ratio close to chondritic, suggest that the spinel crystal was a pre-existing phase (Varela et al., 2002). The possible initial composition of the liquid that could have crystallized the spinel in situ after entrapment (e.g., SiO_2: 32.1 wt%, Al_2O_3: 40.7 wt%, MgO: 13.7 wt%) has not been observed in any spinel-free inclusions (Fuchs et al., 1973). In addition, the fact that in the Murchison chondrite euhedral spinel crystals (Fe and Cr-free) were found within olivines that are not associated with glass inclusions, led Fuchs et al. (1973) to suggest that spinel could pre-date the formation of both, glass inclusions and olivines. Later, McSween (1977) and Varela et al. (2002) suggested that spinels are not daughter crystals formed after entrapment of the glass inclusion, but were trapped as crystals and could have acted as nuclei for the formation of glass inclusion by condensation (as spinel has a condensation temperature, which is clearly higher—1503 K—than that of olivine—1443 K for $p_{tot} \sim 10^{-3}$ atm, Yoneda and Grossman, 1995).

In some inclusions located near a fracture, at temperatures close to 1200 °C, there was an abrupt increase in the bubble size, which continued to grow until the whole inclusion was completely dark (similar to what can be observed during decrepitation). Apparently, the glass did acquired enough mobility to flow out of the cavity leaving an empty void. However, in the majority of the heated glass inclusions, no movement of the bubble was detectable and no change in its shape—even at a temperature of 1450 °C.

Table 3
Major element composition of glasses of heated glass inclusions in olivines (EMPA in wt%)

1100 °C						#h	h	h		Mean
SiO_2	50.2	57.4	50.0	52.4	47.7	49.5	53.2	52.0	55.1	51.9
TiO_2	1.34	0.55	1.32	2.16	1.33	1.33	0.66	0.96	0.46	1.12
Al_2O_3	18.3	14.6	22.1	18.2	20.2	17.1	17.7	18.1	16.5	18.1
Cr_2O_3	0.28	0.47	1.32	0.27	0.23	0.27	0.34	0.18	0.41	0.42
FeO	2.47	3.21	2.23	2.05	4.55	2.00	4.07	3.55	3.33	3.05
MnO	0.09	0.10	0.17	0.09	0.34	0.06	0.13	0.10	0.18	0.14
MgO	9.5	12.3	7.6	7.3	7.2	9.9	9.2	7.4	10.9	9.0
CaO	14.7	9.4	9.3	11.2	11.3	15.1	12.0	11.6	13.1	11.9
Na_2O	2.76	3.35	6.7	5.6	6.3	4.96	1.41	6.2	0.07	4.15
K_2O	0.30	<dl	0.63	0.44	0.64	<dl	0.24	0.03	<dl	0.38
P_2O_5	0.08	<dl	0.05	0.22	0.10	<dl	<dl	<dl	<dl	0.11
Total	100.0	101.3	101.3	99.9	99.7	100.2	98.8	100.1	100.0	100.3
CaO/Al_2O_3	*0.81*	*0.64*	*0.42*	*0.61*	*0.56*	*0.88*	*0.68*	*0.64*	*0.79*	*0.66*
Olivine										
FeO						*4.83*	*8.34*	*8.37*		
MgO						*54.2*	*50.8*	*51.5*		
CaO						*0.28*	*0.21*	*0.19*		

1250 °C	○	○	°h	○	°h	∗	∗h	Mean
SiO_2	50.5	47.3	49.6	50.2	50.2	63.4	61.6	53.3
TiO_2	0.70	0.30	1.75	1.79	0.83	0.42	0.37	0.88
Al_2O_3	14.6	14.9	21.3	21.0	19.3	12.2	9.5	16.1
Cr_2O_3	0.56	0.22	0.17	0.17	0.58	0.10	0.26	0.29
FeO	5.2	8.8	3.76	3.77	2.76	2.23	6.3	4.69
MnO	<dl	0.17	0.07	0.05	0.06	0.07	0.13	0.09
MgO	9.7	5.8	11.9	11.9	7.8	15.2	14.0	10.9
CaO	12.3	17.1	7.6	7.9	11.8	7.6	6.8	10.1
Na_2O	5.1	4.80	2.88	2.92	7.8	<dl	<dl	3.36
K_2O	<dl	<dl	0.63	0.64	0.14	<dl	<dl	0.47
P_2O_5	0.49	<dl	0.74	0.72	<dl	<dl	0.11	0.51
Total	99.2	99.5	100.3	101.0	101.2	101.1	99.1	100.7
CaO/Al_2O_3	*0.84*	*1.15*	*0.36*	*0.38*	*0.61*	*0.62*	*0.71*	*0.63*
Olivine								
FeO			*3.13*		*3.73*		*7.18*	
MgO			*56.5*		*55.6*		*52.3*	
CaO			*0.33*		*0.21*		*0.13*	

1250 °C–24 h					h	h	h	Mean
SiO_2	46.2	46.9	50.1	53.9	51.8	50.5	51.1	50.1
TiO_2	0.85	2.84	1.98	0.84	0.55	0.70	0.74	1.21
Al_2O_3	12.8	13.7	14.5	20.4	12.5	14.6	16.2	15.0
Cr_2O_3	0.70	0.79	0.13	0.07	0.30	0.56	0.37	0.42
FeO	9.1	7.8	6.3	4.2	12.2	5.2	10.0	7.8
MnO	0.10	<dl	0.49	<dl	0.15	0.16	0.14	0.21
MgO	19.4	10.5	8.1	5.7	12.0	9.7	11.6	11.0
CaO	5.4	14.6	15.3	6.9	9.5	12.3	9.9	10.5
Na_2O	5.03	2.16	2.76	6.81	<dl	5.14	<dl	3.13
K_2O	<dl	<dl	0.13	0.87	0.03	<dl	<dl	0.26
P_2O_5	0.24	0.48	<dl	0.16	0.22	0.49	0.04	0.23
Total	99.7	99.8	99.7	99.8	99.3	99.4	100.0	99.8
CaO/Al_2O_3	*0.42*	*1.06*	*1.06*	*0.34*	*0.76*	*0.84*	*0.61*	*0.70*
Olivine								
FeO					*13.1*	*5.8*	*10.8*	
MgO					*47.7*	*53.5*	*49.9*	
CaO					*0.12*	*0.28*	*0.27*	

Table 3 (*continued*)

1450 °C				h	h	Mean
SiO_2	69.6	53.3	52.5	46.9	39.9	52.4
TiO_2	0.24	0.89	0.46	1.86	1.48	0.99
Al_2O_3	8.3	13.2	16.0	17.6	14.7	14.0
Cr_2O_3	0.30	0.56	0.85	0.43	0.27	0.48
FeO	2.37	6.0	4.95	9.5	11.0	6.8
MnO	<dl	0.42	<dl	0.16	0.15	0.24
MgO	9.7	10.2	11.6	9.6	11.3	10.5
CaO	8.4	12.9	11.7	12.2	11.2	11.3
Na_2O	<dl	0.98	0.16	0.15	4.80	1.52
K_2O	0.15	<dl	0.04	0.03	0.11	0.08
P_2O_5	<dl	0.24	0.33	0.05	6.70	1.83
Total	99.0	98.7	98.6	98.5	101.6	100.1
CaO/Al_2O_3	*1.01*	*0.98*	*0.73*	*0.69*	*0.76*	*0.81*
Olivine						
FeO				*9.8*	*12.4*	
MgO				*50.3*	*48.8*	
CaO				*0.22*	*0.32*	

References: #, glass in coexistence with cpx and spinel (Fig. 3a and b), ◦ and ∗, glasses corresponding to two heated objects; h, glass where the composition of the host olivine was measured, <dl, below detection limit.

In a similar range of temperature (between 1200 and 1300 °C) Fuchs et al. (1973) observed a shift in the bubble position of some inclusions suggestive also of a local low liquidus while other glass inclusions located in the same olivine have experienced no movement in the bubble, even after heating to 1400 °C.

Comparison with previous heating experiments suggests that the conditions under which the glass inclusions in olivines of the oxidized CV3 Allende chondrite formed (e.g., estimation of the glass liquidus, presence of pre-existing phases at the moment of formation of the inclusions, etc.), do not differ form those prevailing during formation of glass inclusions in the olivines of a CM chondrite, despite the different chemical composition of their host olivines (e.g., Brearley, 1995; Simon et al., 1995).

4.2. Major chemical composition of heated glasses

Heating experiments aim to reverse the post-entrapment processes that took place inside inclusions during cooling. As the first phase to crystallize onto the inclusions walls during cooling is the host mineral itself, the laboratory heating experiments reverse this process and bring the glass inclusions and its host to a state very close to that when entrapment occurred. Several studies devoted to explore post-entrapment reactions as well as the efficiency of the host as isolator in terrestrial rocks (e.g., Watson, 1976; Quin et al., 1992; Sobolev and Danyushevsky, 1994; Gaetani and Watson, 2000) showed that for slow-diffusing incompatible (with respect to the host olivine) trace elements, the assumption that the glass can be chemical isolated from the external system is valid. However, the composition of the glass with respect to readily exchangeable major elements such as Fe and Mg seems to be vulnerable to post-entrapment modifications.

Heating experiments performed on glass inclusions in olivines of the Allende CV3 chondrite show that the major variations in the chemical composition of the heated glass is mainly related to the two major elements, Fe and Mg. Due to dissolution of the host olivine in the melt, the initially low content of MgO and (FeO) measured in the unheated glass (MgO: 1.59 wt%, FeO: 0.86 wt%, Mean composition, Table 2), can reach values of 9 wt%, (3.05 wt%) and 10.5 wt%, (6.8 wt%) for glass inclusions heated to 1100 and 1450 °C, respectively (mean compositions, Table 3). The binary diagram MgO vs. FeO (Fig. 3a and b) shows that, for glasses enclosed in glass inclusions heated to the same final temperature (e.g., 1250 °C–24 h), the content of FeO in the glass covers a wider range (from 4 to 12 wt%) than that of MgO (from 5.7 to 11.6 wt%, except for one glass inclusion). The same variation is observed in those glasses of glass inclusions which were heated to 1450 °C. In the case of the mesostasis, all have their MgO contents varying between 10 and 15 wt% and a much wider variation in the FeO content (from 3 to 13 wt%), except for two glasses that showed very low contents of both elements. Apparently, for samples heated above 1100 °C, the content of MgO in the glasses (glass inclusions and mesostasis) seems to reach a plateau (close to 15 wt% MgO, with exception of one glass inclusion), despite the different final temperatures to which the sample was heated.

Dissolution of the surrounding olivine and its addition to the initially Si–Al–Ca composition of the glass of the inclusion will also modify the CaO content of glasses (Fig. 3c and d). Although the negative correlation between both elements is slightly developed in glass inclusion glasses, it is also well noticeable in mesostasis glasses (e.g., I cannot exclude dissolution of small low-Ca pyroxenes, Fig. 3d), where for a variation in the MgO content from 0 to 15 wt%, that of CaO covers a range from 18 to 7 wt%. A similar situation occurs with the FeO and CaO contents (Fig. 3e and f). While glasses of glass inclusions appear not to follow any specific correlation, those of the mesostasis show a constant decrease in the CaO content for samples heated to a final temperature of 1100 °C. From

Table 4
Major element composition of heated glassy mesostasis (EMPA in wt%)

1100 °C						Mean
SiO_2	54.0	46.2	53.7	48.4	54.4	51.3
TiO_2	0.74	0.06	0.42	0.1	0.87	0.44
Al_2O_3	17.1	33.6	16.9	30.2	16.5	22.9
Cr_2O_3	0.33	0.04	0.44	0.12	0.35	0.26
FeO	3.93	0.62	4.43	1.15	4.75	2.98
MnO	0.11	<dl	0.11	0.03	0.12	0.09
MgO	10.1	0.4	10.4	2.3	9.9	6.6
CaO	11.6	18.1	11.9	16.7	10.6	13.8
Na_2O	1.36	1.04	1.09	1.28	1.43	1.24
K_2O	0.27	<dl	0.16	0.07	0.29	0.20
P_2O_5	0.03	<dl	<dl	<dl	0.03	0.03
Total	99.6	100.0	99.6	100.3	99.2	99.8
CaO/Al_2O_3	0.68	*0.54*	*0.71*	*0.55*	*0.64*	*0.60*
Olivine						
FeO	8.3	*6.7*		*8.3*	*7.2*	
MgO	51.5	*52.7*		*51.5*	*51.1*	
CaO	*0.23*	*0.25*		*0.23*	*0.22*	

1250 °C	○	○	○	∗	Mean
SiO_2	51.5	48.3	45.6	64.8	52.6
TiO_2	0.47	0.67	0.63	0.44	0.55
Al_2O_3	12.9	17.6	17.6	11.5	14.9
Cr_2O_3	0.52	0.38	0.16	0.15	0.30
FeO	12.6	9.1	12.3	3.0	9.3
MnO	0.65	0.16	0.17	0.06	0.26
MgO	10.3	12.3	11.1	13.8	11.9
CaO	10.6	12.4	12.3	6.9	10.6
Na_2O	0.23	<dl	<dl	<dl	0.23
K_2O	0.16	0.04	<dl	<dl	0.10
P_2O_5	<dl	0.14	0.24	<dl	0.19
Total	99.9	101.1	100.2	100.7	100.7
CaO/Al_2O_3	0.82	*0.70*	*0.70*	*0.60*	*0.71*
Olivine					
FeO		*3.8*	*6.0*		
MgO		*55.9*	*53.6*		
CaO		*0.27*	*0.2*		
Olivine					
FeO		*4.34*	*8.7*		
MgO		*55.3*	*51.6*		
CaO		*0.25*	*0.19*		
Olivine					
FeO			*8.4*		
MgO			*51.8*		
CaO			*0.2*		

1250 °C–24 h				Mean
SiO_2	52.0	52.2	51.8	52.0
TiO_2	0.70	0.62	0.59	0.64
Al_2O_3	14.4	14.1	13.3	13.9
Cr_2O_3	0.32	0.34	0.34	0.33
FeO	10.3	9.7	13.1	11.0
MnO	0.18	0.16	0.21	0.18
MgO	13.4	13.8	11.7	13.0
CaO	9.5	9.4	9.1	9.3
Na_2O	<dl	<dl	<dl	<dl
K_2O	<dl	<dl	<dl	<dl
P_2O_5	0.13	0.06	<dl	0.10

Table 4 (*continued*)

1250 °C–24 h					Mean
Total	101.0	100.4	100.1		100.5
CaO/Al_2O_3	*0.66*	*0.66*	*0.69*		*0.67*
Olivine					
FeO	12.1	*12.1*	*16.4*		
MgO	47.8	*48.0*	*44.8*		
CaO	0.2	*0.20*	*0.26*		

1450 °C							Mean
SiO_2	52.2	53.6	51.8	50.2	52.9	50.6	51.9
TiO_2	0.52	0.65	0.61	0.43	0.39	0.88	0.58
Al_2O_3	13.6	13.4	14.3	14.7	13.5	12.9	13.7
Cr_2O_3	0.50	0.32	0.47	0.27	0.69	0.15	0.40
FeO	7.8	8.2	8.4	9.8	8.5	11.2	9.0
MnO	0.10	0.14	0.14	0.62	0.11	0.00	0.19
MgO	15.1	13.7	14.7	12.3	11.7	9.3	12.8
CaO	8.8	10.1	9.5	10.6	11.8	12.6	10.6
Na_2O	<dl	<dl	<dl	0.63	0.35	1.24	0.56
K_2O	<dl	0.03	<dl	<dl	0.06	<dl	0.05
P_2O_5	<dl	0.10	<dl	<dl	0.10	0.42	0.16
Total	98.5	100.2	100.1	99.5	100.0	99.3	99.9
CaO/Al_2O_3	*0.65*	*0.75*	*0.66*	*0.72*	0.87	0.98	*0.77*
Olivine							
FeO			*9.2*	*9.9*	*9.9*	*13.1*	
MgO			*49.7*	*45.2*	*45.2*	*43.2*	
CaO			*0.25*	*0.33*	*0.33*	*0.29*	

References: ° and ∗, glasses corresponding to two heated objects; <dl, below detection limit.

that temperature on, the CaO contents in glasses cluster, covering a narrow range: from ~9 to 12 wt% CaO and from ~8 to 13 wt% in FeO. The content of both elements appears not to be correlated with the final temperature to which the sample is heated. If the content of FeO + MgO is compared to that of Al_2O_3 (Fig. 3g and h), glasses of glass inclusions show a slight negative correlation, better developed in samples heated to 1250 °C during 24 h. The content of the three elements in the mesostasis glass appear also to cluster (with exception of two data) around 18 and 12 wt% Al_2O_3 and around ~14 and 25 wt% FeO + MgO. Because these compositions (Fe, Ca and Al) cluster rather than show continuous mixing, they appear to have been buffered by conditions establish during heating.

4.3. The Ca and Al content of glasses

Apparently the CaO and Al_2O_3 content of the mesostasis seems to have acquired or approached equilibrium under the situation created by the heating experiments. While the CaO and Al_2O_3 contents of glasses of glass inclusions show super- and sub-chondritic CaO/Al_2O_3ratios, those of the mesostasis (with the exception of two data) cluster tightly around the chondritic value (Fig. 3i and j). If Ca and Fe–Mg partitioning between olivine and glass is compared, the values of the heated glasses of the mesostasis (open symbols in Fig. 4) are mainly (exception of five data) close to, or comprised in, the expected range for a crystal/liquid

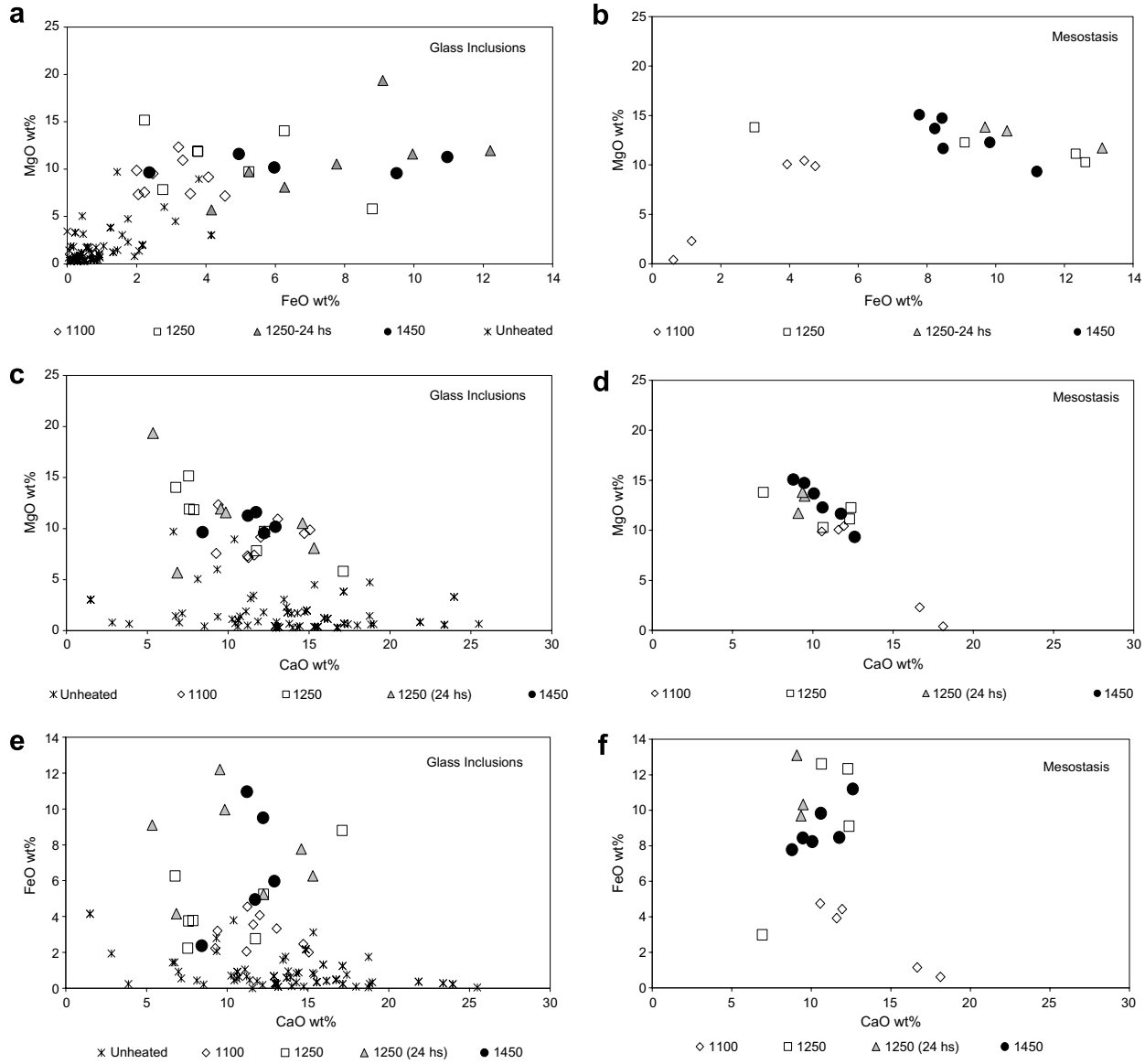

Fig. 3. (a) MgO vs. FeO contents of unheated and heated glass inclusions in olivine and (b) heated mesostasis glass. For samples heated above 1100 °C, the content of MgO in the all types of glasses is below 15 wt%. (c) MgO vs. CaO contents of unheated and heated glass inclusions in olivine and (d) heated mesostasis glass. Note the well-developed anti-correlation in mesostasis glasses. (e) FeO vs. CaO contents of unheated and heated glass inclusions in olivine and (f) heated mesostasis glass. Note that heated mesostasis glass shows a constant decrease in the CaO and increase in FeO contents for samples heated to a final temperature of 1100 °C, and from that temperature on, the CaO contents in glasses clusters, covering a narrow range. (g) FeO + MgO vs. Al_2O_3 contents of unheated and heated glass inclusions in olivine and (h) heated mesostasis glass. The contents of the three elements in the mesostasis glass appear also to cluster. (i) CaO vs. Al_2O_3 contents of unheated and heated glass inclusions in olivine and (j) heated mesostasis glass. Unheated glass inclusions show mainly sub-chondritic Ca/Al ratios while the heated ones cover a wide range in the CaO and Al_2O_3 contents showing sub- and super-chondritic ratios. Glasses of the heated mesostasis cluster tightly close to the chondritic value. (k) Na_2O vs. SiO_2 contents of unheated and heated glass inclusions in olivine and (l) heated mesostasis glass. Sodium appears to have been preserved in glasses enclosed in glass inclusions (with exception of those samples heated to 1450 °C) but lost in the mesostasis glass.

Ca equilibrium, as determined experimentally (Kennedy et al., 1993; Libourel, 1999). The situation looks different for glasses of glass inclusions in Allende which turn to be more protected by the olivine and thus, are more akin to keep their original content in volatile elements. However, as mesostasis are open systems and therefore more sensible to record the latest conditions to which they have been exposed, the observed results suggest that the chondritic atmosphere—resulting from heating a piece of chondrule or aggregate in which the studied sample was immersed—could have buffered the chemical variation of the heated mesostasis glass composition.

Because the heating experiments can bring phases (e.g., olivine and mesostasis glass) to a condition close

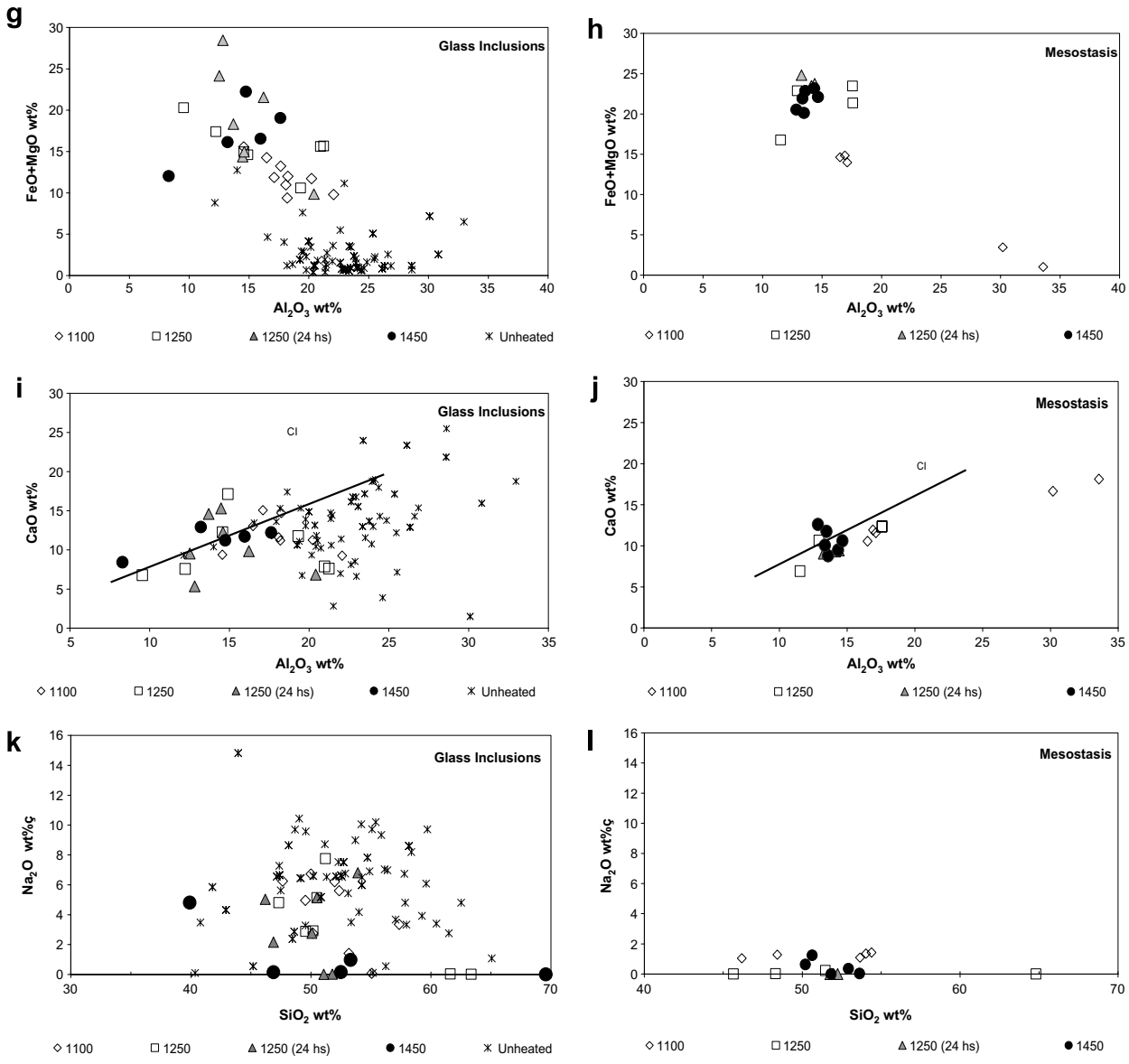

Fig. 3 (*continued*)

to that prevailing during their formation, the Ca contents of the heated glasses of the mesostasis are in the expected range for a crystal/liquid Ca equilibrium. These results are in good agreement to those obtained in unheated pristine phases. As we have previously shown, if conditions are such that the olivine is a primitive high-Ca olivine and the glass keeps its pristine composition (e.g., Ca–Al-rich with Ca/Al chondritic ratio), both phases are in equilibrium with respect to their CaO contents (Varela et al., 2005, 2006). An example of this can also be observed in the unheated clear mesostasis in Allende, where glasses with 18.3 wt% CaO (first analysis, Table 2) and 17.7 wt% (last analysis) are in contact with high-Ca olivine (CaO: 0.52 and 0.47 wt%, respectively) and both phases can reach equilibrium with respect to their CaO contents [Kd(Ca): 0.028 and 0.026, respectively] (Fig. 4).

4.4. Volatile elements

The content of Na_2O in the heated glass inclusions covers the same range as those in the unheated glasses, with exception of glass inclusions that were heated to a final temperature of 1450 °C, and the glass from the mesostasis (Fig. 3k and l), which apparently lost Na at that high temperature. Evidently, glass inclusions can behave as closed systems and preserved the alkalis they acquired presumably in the nebula. An example is observed in the multiphase glass inclusions heated to a final temperature of 1100 °C, where a fibrous crystal did form. The newly formed clinopyroxene (Na_2O: 1.07 wt%) coexists with the glass (Na_2O: 4.96 wt%) of the multiphase glass inclusion, which is hosted by an olivine Fo_{95} (SiO_2: 41.8 wt%, MgO: 54.2 wt%, CaO: 0.28 wt%, FeO: 4.83 wt%). The apparently high Na distribution between clinopyroxene and liquid of 0.216, which

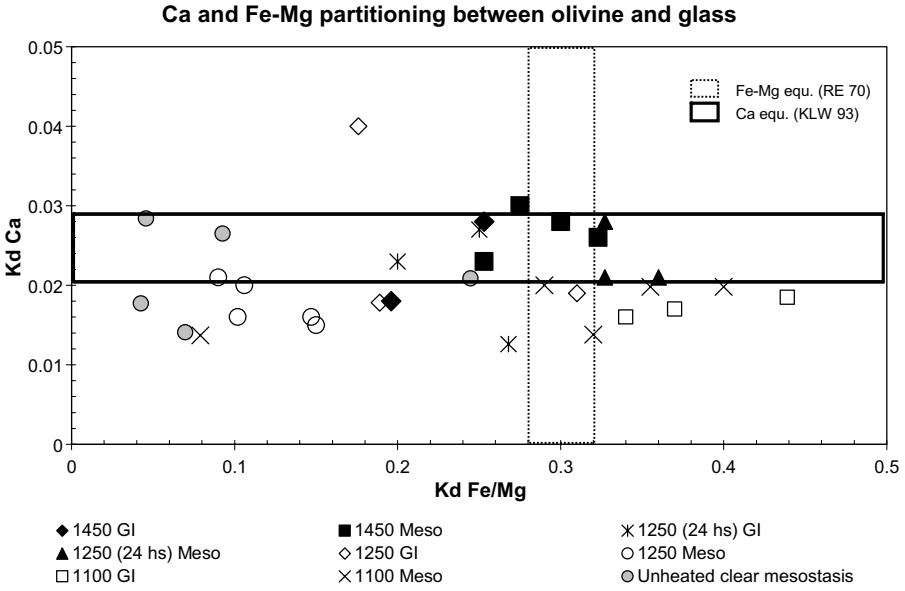

Fig. 4. Ca and Fe–Mg partitioning between olivine and glass. Note that heated mesostasis glasses are close to or within the range established by Ca experimental equilibrium conditions (horizontal area with bold line). Vertical area corresponds to equilibrium conditions with respect to the Fe–Mg exchange between olivine and glass. RE 70: Roeder and Emslie (1970), KWL 93: Kennedy et al. (1993). Unheated data—from a rare clear mesostasis—are also shown.

lies above the Na contents of mesostasis and clinopyroxene pairs in type I and type II chondrules (Jones, 1990, 1994, 1996; Alexander and Grossman, 2005), could be suggestive of its low temperature formation. As has been indicated by the thermodynamic modeling of the Na distribution (Blundy et al., 1995), there should be a significant temperature dependence of the distribution coefficient, which can increase from 0.04 at ~1573 K, to 0.1 at ~1273 K, and 0.2 at ~1173 K. The changes observed inside the glass inclusion during heating (e.g., variation in the bubble size at 950 °C and formation of the clinopyroxene before the final temperature of 1100 °C) and the estimated Na distribution coefficient of 0.216 for the newly formed clinopyroxene and its coexisting glass, are in good agreement with model predictions for clinopyroxenes formed at low temperatures. Clearly, the assemblage of phases enclosed by the glass inclusion in the host crystal can be chemically sealed.

As we have previously shown, all glasses of the primary glass inclusions in olivine have a Si–Al–Ca-rich composition, with about chondritic CaO/Al_2O_3 and Al_2O_3/TiO_2 ratios (Varela et al., 2002a,b, 2005). These glasses will plot inside the area of the ellipse GI (Fig. 5a) as do also the glasses of the clear mesostasis. However, the Na-rich glasses have similar contents of Al_2O_3 but have lower contents of CaO (Fig. 5a) indicating that Na-rich glasses could have been derived by loss of Ca and gain of Na. This variation—in this pristine chemical composition were glasses can acquire Na^+ and K^+ (and other alkalis) for Ca^{2+}—indicates that secondary elemental exchange reactions took place (Varela et al., 2002a, 2005, 2006). The Na_2O vs. CaO anti-correlation that covers the area of the ellipse GO (acronym of Glass Open, Fig. 5a) is mainly observed in glasses that have acted as open systems, were this exchange reaction was studied in detail (e.g., glass inclusions touched by fractures in CR chondrites—Varela et al., 2002a—neck inclusions (inclusions, which are still connected to the mesostasis) and mesostasis in CV3 chondrites and BO chondrules—Varela et al., 2005, 2006). The unheated glasses of glass inclusions in Allende cover the same areas as define by the previous studies and, in addition, define two extra trends showing low (line 1, Fig. 5a) and high (ellipse in bold, Fig. 5a) CaO contents, respectively. Interestingly, all compositional glass trends preserve a good anti-correlation of Na_2O and CaO contents.

Since the content of Na_2O in the heated glass inclusions could be kept (with exception of glass inclusions that were heated to a final temperature of 1450 °C, Figs. 3k and 5b), these objects apparently behaved as closed systems with respect to alkali elements.

If this is so, variation in the alkali content of glasses during heating experiment can bring some light onto the ongoing discussion about their role in the chondrule formation process.

Because the alkali content of the mesostasis glass can be erased if those objects are heated to temperatures higher than 1100 °C (Fig. 3k and l), but that of the mesostasis glass of chondrules and aggregates available to us are rich in alkalis, the process under which Na was incorporated in glasses must have been a low temperature one, e.g., it must have taken place at sub-solidus conditions. In addition, the absence of alkali evaporation is also supported by a K isotope study of glass mesostasis and glass inclusions in Bishunpur chondrules (Alexander et al., 2000) that clearly showed that no K isotope Rayleigh mass fractionation had taken place. Moreover, K isotope fractionation is absent in the glass inclusions as well as in the mesostasis.

Experimental studies of evaporation and isotopic mass fractionation of potassium in silicate melts (Yu et al.,

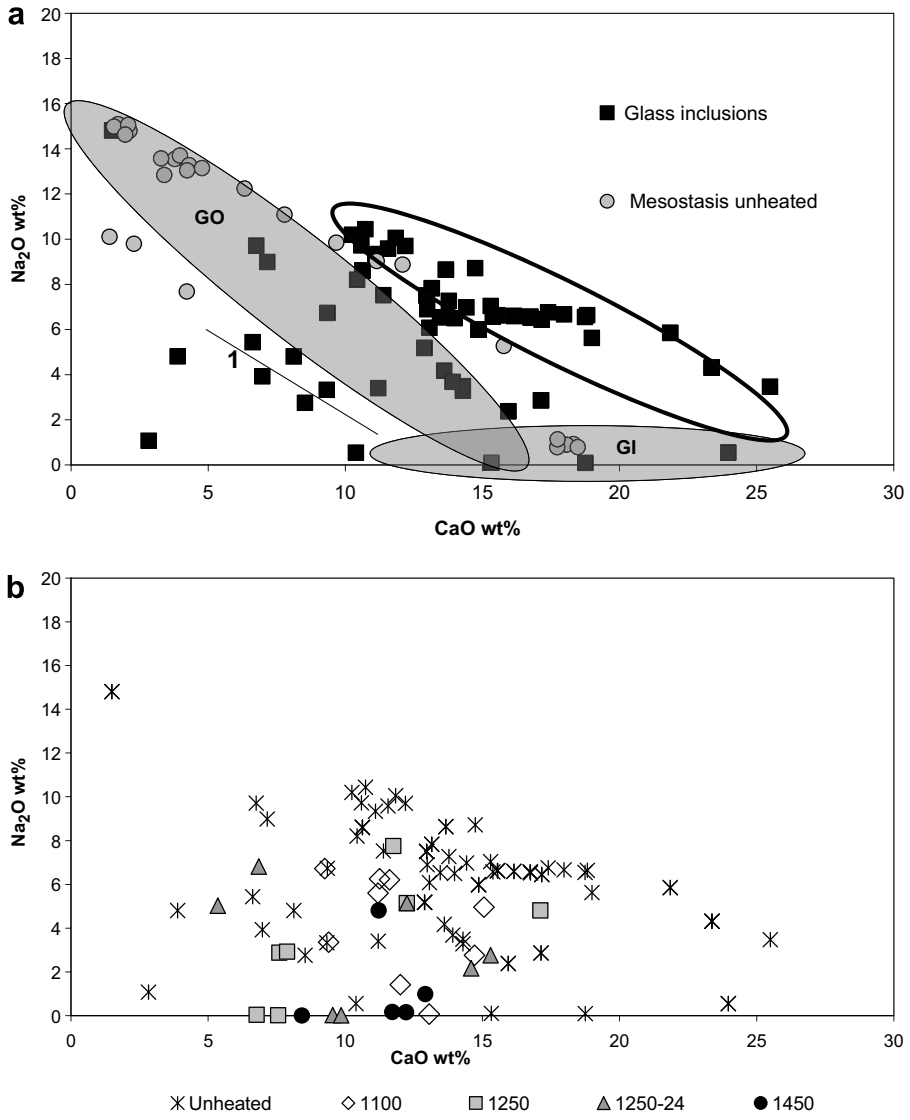

Fig. 5. (a) Na_2O vs. CaO contents of unheated glass inclusions in olivine and mesostasis of Allende meteorite. The two ellipses show the areas cover by glasses of glass inclusions (ellipse named as GI) and for glasses of neck inclusions, mesostasis and glass inclusions reached by fractures (ellipse named GO, acronym of Glass Open) in the CR, CM and the Kaba CV3 chondrites, respectively (Varela et al., 2002, 2005). The Allende glass inclusion data fit these areas and define two new trends: a low CaO content glass group (line 1) and a high CaO content one (ellipse with bold line). The unheated clear mesostasis glass has a high content of Al_2O_3 and a very low Na_2O content, plots into the GI ellipse. The re-crystallized mesostasis analyses plot into both ellipses and in the trend define by line 1. All of these data show a Na_2O vs. CaO negative correlation. (b) Na_2O vs. CaO contents of unheated and heated glass inclusions in olivine of Allende meteorite.

2002) show that $\delta^{41}K$ decreases with increasing pressure, because of back reactions between the melt and K in the gas. In a recent study of alkali elemental and potassium isotopic composition of Semarkona chondrules, Alexander and Grossman (2005) suggest that the lack of systematic isotopic enrichments observed in its chondrules, even in the alkali depleted type I, is that they exchanged with the ambient gas as they cooled.

Evidently, all available results point towards alkalis being introduced by a low temperature process. One of the possible mechanisms could be fluid circulation (e.g., during metasomatism) in a parent body. However, the absence of signs of devitrification in the glasses of Na-rich glass inclusions and mesostasis makes this process difficult to be considered as being responsible for the observed Na–Ca replacement. Also, and as was indicated in the study of glasses in the Kaba CV3 chondrite (Varela et al., 2005), the matrix is too poor in alkalis (Na_2O: 0.78 wt% for Kaba matrix, Scott et al., 1988) to create a compositional potential capable to pump up to the high contents of Na_2O observed in the glass (>10 wt%).

The Na_2O vs. CaO anti-correlation shown by glasses of chondrules and aggregates of primitive chondrites has been interpreted (Kurat, 1967, 1988; Varela et al., 2002; Varela et al., 2005; Varela et al., 2006) to be the result of a vapor–glass exchange reaction in which Ca in the glass

was replaced by Na from the vapor. All indices—including the heating experiments reported here—show that a liquid mesostasis–vapor exchange (e.g., Libourel et al., 2006) is not feasible. According to the Primary Liquid Condensation Model (Varela et al., 2005) calcium that acts mainly as a network modifier cation can be easily exchanged for alkali elements (Na, Li, Rb) at sub-solidus temperatures. As previously explained, one possible way this exchange can occur is following the Modifier Random Network (MRN) model of Greaves (1985). Under the MRN the structure of liquids (melts) as well as their frozen derivatives, glasses, consists of differently oriented amorphous regions (islands) with high concentrations of network formers which contain "percolation channels" with high concentrations of network modifiers and non-bridging oxygens that provide a high degree of mobility to these ions. Thus, a continuing communication of the chondrules and aggregates with the cooling nebula at sub-solidus temperatures, as proposed by the Primary Liquid Condensation Model (Varela et al., 2005, 2006) appears to be the mechanism that is indicated by the data available today.

Interestingly, the CaO and Al_2O_3 contents of the heated mesostasis glass of the Allende CV3 chondrite cluster around chondritic values. The preferred explanation for this result, as mentioned above, is that the chondritic atmosphere could have buffered the chemical variation of the heated mesostasis glass composition. This seems also to be supported by the fact that the Ca contents of the heated glasses of the mesostasis are in the expected range for a crystal/liquid Ca equilibrium. Thus, as shown by these experiments, the Ca-exchange reaction between a gas and a phase at sub-solidus temperatures can effectively take place in a short time.

5. CONCLUSIONS

Heating experiments performed on glasses of glass inclusions in olivines and mesostasis of aggregates of the Allende CV3 chondrite up to final temperatures of 1100, 1250 and 1450 °C show that glasses can keep valuable information concerning those elements that are incompatible to the host olivine (e.g., Na, Al and Ca).

Unheated mesostasis and inclusion glasses in carbonaceous chondrites differ in their chemical composition (e.g., in their Na_2O content) according to their behavior as open or close systems, respectively. In the first case, the primary glass inclusions in olivine have a Si–Al–Ca-rich composition and an approximately chondritic Ca/Al ratio. In the second, the mesostasis (and/or neck inclusions and glass inclusions reached by fractures) can be Na-rich with a sub-chondritic Ca/Al ratio. This ratio is a consequence of the Ca–Na exchange with the vapor which led to low Ca contents without changing the original content of Al_2O_3.

The Ca contents of the heated glasses of the mesostasis are in the expected range for a crystal/liquid Ca equilibrium and these experiments prove that the Ca-exchange reaction between a gas and a phase at sub-solidus temperatures can effectively take place in a short time.

Glasses of glass inclusions are more akin to keep their original content in volatile elements while that of the mesostasis glass can be altered if the objects are heated to temperatures higher than 1100 °C. Sodium is quickly lost above this temperature in the experiments, which indicates that the process under which Na was incorporated into glasses of the objects available to us must have been a low temperature one. The absence of signs of devitrification—that could be expected if fluid circulation takes place—as well as the presence of a Na_2O vs. CaO anti-correlation in the glasses of Na-rich glass inclusions and mesostasis, favor the Na–Ca replacement within the cooling nebula at sub-solidus temperatures as the mechanism responsible for the alkali enrichment in glasses of meteorites.

ACKNOWLEDGMENTS

I thank Roberto Clocchiatti and Dominique Massare for the invaluable help they provided during laboratory work and for their constant advices for glass inclusions studies and Gero Kurat for support and discussions. The thorough reviews of Guy Libourel and Alexander Krot (associated editor) helped to improve the manuscript. Financial support was received from Laboratory Pierre Süe, France, FWF (P16420-N10), Austria, CONICET (PIP 5005) and CONICET-FWF International Cooperation Project, Argentina.

REFERENCES

Alexander C. M. O'D. and Grossman J. N. (2005) Alkali elemental and potassium isotopic compositions of Semarkona chondrules. *Meteoritics Planet. Sci.* **40**, 541–556.

Alexander C. M. O'D., Grossman J. N., Wang J., Zanda B., Bourot-Denise M. and Hewins R. H. (2000) The lack of potassium-isotopic fractionation in Bishunpur chondrules. *Meteoritics Planet. Sci.* **35**, 856–868.

Blundy J. D., Fallon T. J., Wood B. J. and Dalton J. A. (1995) Sodium partitioning between clinopyroxene and silicate melts. *J. Geophys. Res. B* **100**, 15501–15515.

Brearley A. J. (1995) Aqueous alteration and brecciation in Bells, an unusual, saponite-bearing CM carbonaceous chondrite. *Geochim. Cosmochim. Acta* **59**, 2291–2317.

Clocchiatti R. and Massare D. (1985) Experimental crystal growth in glass inclusions: the possibilities and the limits of the method. *Contrib. Mineral. Petrol.* **89**, 193–204.

Fuchs L. H., Olsen E. and Jensen K. J. (1973) Mineralogy, mineral–chemistry and composition of the Murchison (C2) meteorite. *Smithson. Contrib. Earth Sci.* **10**, 38.

Gaetani G. A. and Watson E. B. (2000) Open system behaviour of olivine-hosted melt inclusions. *Earth Planet. Sci. Lett.* **183**, 27–41.

Greaves G. N. (1985) EXAFS and the structure of glass. *J. Non-Cryst. Solids* **71**, 203–217.

Ikeda Y. and Kimura M. (1995) Anhydrous alteration of Allende chondrules in the solar nebula I: description and alteration of chondrules with known oxygen-isotopic composition. *Proc. NIPR Symp. Antarctic Meteorites* **8**, 97–122.

Jones R. H. (1990) Petrology and mineralogy of type II, FeO-rich chondrules in Semarkona (LL3.0): origin by closed-system fractional crystallization with evidence for supercooling. *Geochim. Cosmochim. Acta* **54**, 1785–1802.

Jones R. H. (1994) Petrology of FeO-poor, porphyritic pyroxene chondrules in the Semarkona meteorite. *Geochim. Cosmochim. Acta* **58**, 5325–5340.

Jones R. H. (1996) FeO-rich porphyritic pyroxene chondrules in unequilibrated ordinary chondrites. *Geochim. Cosmochim. Acta* **60**, 3115–3138.

Kennedy A. K., Lofgren G. E. and Wasserburg G. J. (1993) An experimental study of trace element partitioning between olivine, orthopyroxene and melt in chondrules: equilibrium values and kinetics effects. *Earth Planet. Sci. Lett.* **115**, 177–195.

Kurat G. (1967) Einige Chondren aus dem Meteoriten von Mezö-Madaras. *Geochim. Cosmochim. Acta* **31**, 1843–1857.

Kurat G. (1988) Primitive meteorites: an attempt towards unification. *Philos. Trans. R. Soc. Lond.* **A325**, 459–482.

Libourel G. (1999) Systematics of calcium partitioning between olivine and silicate melt: implications for melt structure and calcium content of magmatic olivines. *Contrib. Mineral. Petrol.* **136**, 63–80.

Libourel G., Krot A. and Tissandier L. (2006) Role of gas–melt interaction during chondrule formation. *Earth Planet. Sci. Lett.* **251**, 232–240.

Métrich N. and Clocchiatti R. (1989) Melt inclusions investigation of the volatile behaviour in historic basaltic magmas of Etna. *Bull. Volcanol.* **51**, 185–198.

McSween H. (1977) On the nature and origin of isolated olivine grains in carbonaceous chondrites. *Geochim. Cosmochim. Acta* **41**, 411–418.

Quin Z., Lu F. and Anderson A. T. (1992) Diffusive re-equilibration of melt and fluid inclusions. *Am. Mineral.* **77**, 565–576.

Roeder P. L. and Emslie R. F. (1970) Olivine–liquid equilibria. *Contrib. Mineral. Petrol.* **29**, 275–289.

Schiano P. (2003) Primitive mantle magmas recorded as silicate melt inclusions in igneous minerals. *Earth Sci. Rev.* **63**, 121–144.

Scott E. R. D., Barber D. J., Alexander C. M., Hutchison R. and Peck J. A. (1988) Primitive material surviving in chondrites: matrix. In *Meteorites and the Early Solar System* (eds. J. F. Kerridge and M. S. Matthews). University of Arizona Press, pp. 808–818.

Simon S. B., Grossman L., Casanova I., Symes S., Benoit P., Sears D. W. G. and Wacker J. F. (1995) Axtell, a new CV3 chondrite form Texas. *Meteoritics* **30**, 42–46.

Sobolev A. V. and Danyushevsky L. V. (1994) Petrology and geochemistry of boninites from the north termination of the Tonga Trench: constraints on the generation conditions of primary high Ca boninite magmas. *J. Petrol.* **35**, 1183–1211.

Sobolev A.V., Bakumenko I. T. and Kostyuk V. P. (1976) The possibility for using melt inclusions for petrologic conclusions. Akad. Nauk. S.S.S.R., Siberian branch Geol. I Geofiz., 1976, No. 5, 146–149. (In Russian: translated in *Fluid inclusions Research, Proceedings of COFFI,* **9**, 178–181.)

Varela M. E., Kurat G., Mosbah M., Clocchiatti R. and Massare D. (2000) Glass-bearing inclusions in olivine of the Chassigny achondrite: heterogeneous trapping at sub-solidus temperatures. *Meteoritics Planet. Sci.* **35**, 39–52.

Varela M. E., Kurat G., Hoppe P. and Brandstätter F. (2002a) Chemistry of glass inclusions in olivines of the CR chondrite Renazzo, Acfer 182, and El Djouf 001. *Geochim. Cosmochim. Acta* **66**, 1663–1679.

Varela M. E., Kurat G., Hoppe P. and Weisberg M. K. (2002b) Chemistry of glass inclusions in olivines of a Dark Inclusion and the host Allende CV3 chondrite. *XXXIII Lunar and Planet. Sci. Conf.* #1190 (abstr.).

Varela M. E., Kurat G. and Zinner E. (2005) A liquid-supported condensation of major minerals in the solar nebula: evidence from glasses in the Kaba CV3 chondrite. *Icarus* **178**, 553–569.

Varela M. E., Kurat G. and Zinner E. (2006) The primary liquid condensation model and the origin of barred olivine chondrules. *Icarus* **184**, 344–364.

Watson E. B. (1976) Glass inclusions as samples of early magmatic liquid: determinative method and application to a South Atlantic basalt. *J. Volcanol. Geotherm. Res.* **1**, 73–84.

Yoneda S. and Grossman L. (1995) Condensation of Ca–MgO–Al_2O_3–SiO_2 liquids from cosmic gases. *Geochim. Cosmochim. Acta* **59**, 3413–3444.

Yu Y., Hewins R., Alexander C. M. O'D. and Wang J. (2002) Experimental study of evaporation and isotopic mass fractionation of potassium in silicate melts. *Geochim. Cosmochim. Acta* **67**, 773–786.

Zapunnyy S. A., Sobolev A. V., Bogdanov A. A., Slutskiy A. B., Dmitriyev L. V. and Kunin L. L. (1989) An apparatus for high-temperature optical research with controlled oxygen fugacity. *Geochem. Int.* **26**, 120–128.

Associate editor: Alexander N. Krot